European Commission

JRC SCIENTIFIC AND POLICY REPORTS

Fission cross section measurements for ^{240}Pu, ^{242}Pu

Deliverable 1.5 of the ANDES project

P. Salvador-Castiñeira, A. Tsinganis, M. Aiche, S. Andriamonje, G. Belier, E. Berthoumieux, G. Boutoux, T. Brys, M. Calviani, S. Czajkowski, N. Colonna, Q. Ducasse, R. Eykens, C. Guerrero, F. Gunsing, F.-J. Hambsch, B. Jurado, G. Kessedjian, C. Massimi, L. Mathieu, J. Mattaranz, A. Moens, S. Oberstedt, A.J.M. Plompen, C. Pretel, G. Sibbens, J. Taieb, D. Vanleeuw, M. Vidali, V. Vlachoudis, R. Vlastou, the n_TOF Collaboration

2013

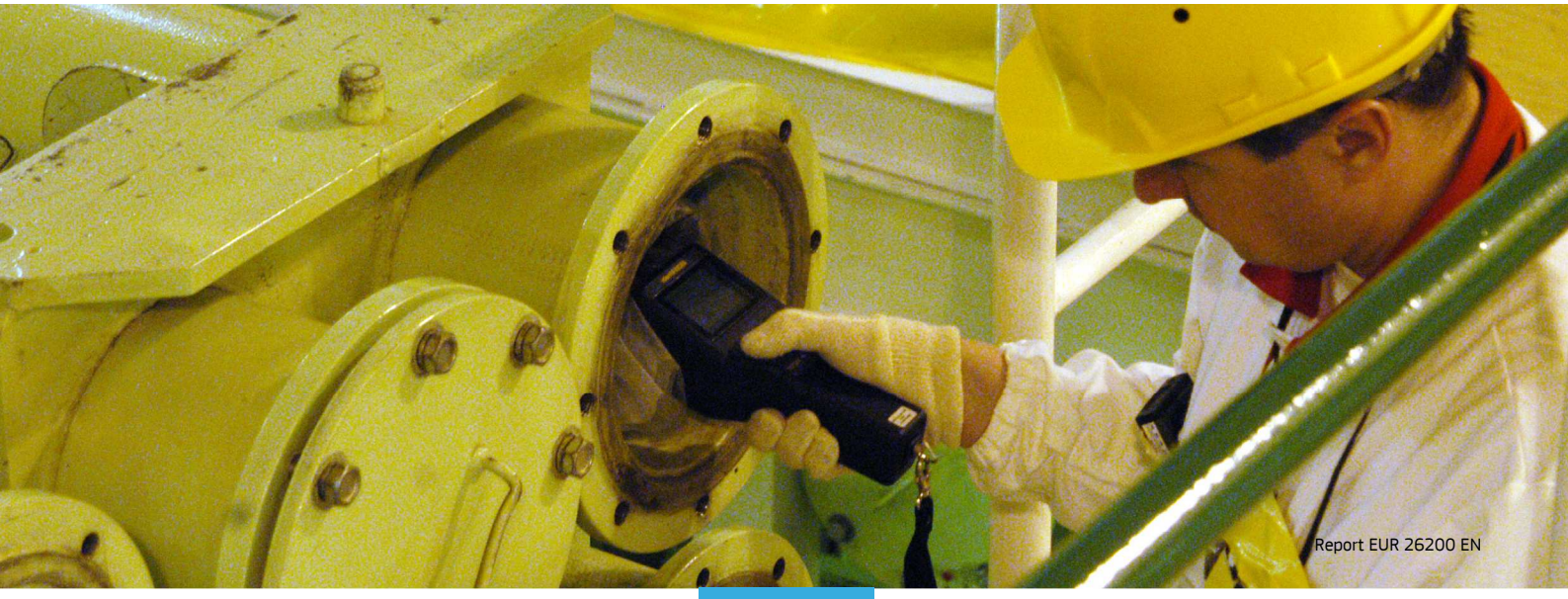

Report EUR 26200 EN

Joint Research Centre

European Commission
Joint Research Centre
Institute for Reference Materials and Measurements

Contact information
Arjan Plompen
Address: Joint Research Centre, Retieseweg 111, 2440 Geel, Belgium
E-mail: Arjan.Plompen@ec.europa.eu
Tel.: +31 14 571 381

http://www.jrc.ec.europa.eu/

JRC 85144

EUR 26200 EN

ISBN 978-92-79-33002-5 (pdf)

ISSN 1831-9424 (online)

doi: 10.2787/81004 (pdf)

Luxembourg: Publications Office of the European Union, 2013

Printed in Belgium

SEVENTH FRAMEWORK PROGRAMME OF THE EUROPEAN ATOMIC ENERGY COMMUNITY

Nuclear Fission and Radiation Protection

Project acronym: ANDES

Project full title: Accurate Nuclear Data for nuclear Energy Sustainability

Grant Agreement no.: FP7 – 249671

Workpackage N°: 1

Identification N°: D1.5

Type of document: Report

Title: Final report on the fission cross section measurements for ^{240,242}Pu

Dissemination Level: Public

Reference: Deliverable D1.5

Status: Final

	Name	Partner	Date	Signature
edited by:	A.J.M. Plompen	JRC	21-10-2013	
WP leader:	A.J.M. Plompen	JRC	21-10-2013	
IP Co-ordinator:	E.M. Gonzalez Romero	CIEMAT	21-10-2013	

Fission cross section measurements for ^{240}Pu, ^{242}Pu

The ANDES deliverable D1.5 of

Work Package 1, Task 3

P. Salvador-Castiñeira[1,2], A. Tsinganis[3,4], M. Aiche[5], S. Andriamonje[4], G. Belier[6], E. Berthoumieux[7], G. Boutoux[6], T. Brys[1], M. Calviani[4], S. Czajkowski[5], N. Colonna[8], Q. Ducasse[5,9], R. Eykens[1], C. Guerrero[4], F. Gunsing[7], F.-J. Hambsch[1], B. Jurado[5], G. Kessedjian[10], C. Massimi[11], L. Mathieu[5], J. Mattaranz[5], A. Moens[1], S. Oberstedt[1], A.J.M. Plompen[1], C. Pretel[2], G. Sibbens[1], J. Taieb[6], D. Vanleeuw[1], M. Vidali[1], V. Vlachoudis[4], R. Vlastou[3], the n_TOF Collaboration[12]

[1] *European Commission, Joint Research Centre,*
Institute for Reference Materials and Measurements,
Retieseweg 111, B-2440 Geel, Belgium.

[2] *Institute of Energy Technologies, Technical University of Catalonia,*
Avda. Diagonal 647, E-08028 Barcelona, Spain

[3] *National Technical University of Athens (NTUA), Greece*

[4] *European Organisation for Nuclear Research (CERN), Geneva, Switzerland*

[5] *CENBG-IN2P3-CNRS, BP120, 33175 Gradignan, France*

[6] *CEA-DAM, SPhN, 91680 Bruyères-le-Châtel, France*

[7] *Commissariat à l'Énergie Atomique (CEA) Saclay - Irfu, Gif-sur-Yvette, France*

[8] *Istituto Nazionale di Fisica Nucleare, Bari, Italy*

[9] *CEA, DEN, DER, F-13108 Saint Paul Lez Durance, France*

[10] *LPSC-IN2P3-CNRS, 53 Avenue des Martyrs, 38026 Grenoble, France*

[11] *Dipartimento di Fisica e Astronomia, Universita' di Bologna, and Sezione INFN di Bologna, Italy*

[12] *www.cern.ch/ntof*

October 24, 2013

Contents

Chapter 1

Measurements of the ^{240,242}Pu(n,f) cross sections

The ANDES "Accurate Nuclear Data for nuclear Energy Sustainability" project (FP7 Euratom contract 249671), Work Package 1 (WP1) , "Measurements for Advanced Reactor Systems", Task 1.3 "High accuracy measurements for fission" has three subtasks committed to measuring the neutron-induced fission cross sections of ^{240}Pu and ^{242}Pu. These measurements differ by measurement principle, flux normalization and neutron source. Moreover in the measurement principles applied they differ from what was done before for these reactions. In this way ANDES aimed to make a substantial new contribution to the knowledge of the neutron-induced fission cross section for these two isotopes. In doing so it reacted to the observations that 1) despite numerous earlier measurements the spread in the data is larger than the target uncertainty established by sensitivity analyses [1, 2, 3, 4, 5, 6], 2) a large number of earlier measurements relies on parallel plate fission ionization chambers in which the Pu samples are back-to-back with ^{235}U for normalization. For a summary of the status prior to the ANDES measurements see Ref. [7].

Subtask 1.3.b concerns measurements with double Frisch-grid ionization chambers in which the fission cross section of ^{240}Pu or ^{242}Pu is measured relative to a flux monitor which is either the fission rate from ^{237}Np or from ^{238}U. The neutrons are produced by binary reactions at the IRMM Van de Graaff accelerator. These measurements are described in chapter 2. The lead partner of this work is IRMM.

Subtask 1.3.c concerns measurements with photovoltaic cells to determine the fission rate of ^{240}Pu and ^{242}, with back-to-back samples and the the neutron fluence rate by means of a proton recoil telescope. Also here quasi mono-energetic neutrons are used. In a first experiment this involved the Van de Graaff accelerator at Bruyeres-le-Châtel. The status of this work is described in chapter 4. The lead partner of this work is CNRS/CENBG.

Subtask 1.3.d concerns measurements with micromegas detectors and the time-of-flight technique at the CERN based n_TOF facility. The setup consists of four detectors for ^{240}Pu, four for ^{242}Pu and two for ^{235}U. The latter two are used for the determination of the neutron fluence rate. The status of this work is described in chapter 3. The lead partner of this work is INFN (Istituto Nazionale di Fisica

Nucleare) sezione Bari and the main partners are NTUA (National Technical University of Athens) and CERN.

The present report is deliverable D1.5 of the ANDES project.

Chapter 2

Measurements of the fission cross sections of ^{240,242}Pu at IRMM

P. Salvador-Castiñeira[1,2], T. Brys[1], R. Eykens[1], F.-J. Hambsch[1], A. Moens[1], S. Oberstedt[1], C. Pretel[2], G. Sibbens[1], D. Vanleeuw[1], M. Vidali[1],

1) European Commission, Joint Research Centre, Institute for Reference Materials and Measurements (JRC-IRMM), Retieseweg 111, B-2440 Geel, Belgium

2) Institute of Energy Technologies, Technical University of Catalonia, Avda. Diagonal 647, E-08028 Barcelona, Spain

Abstract

Fast spectrum neutron-induced fission cross-section data for transuranic isotopes are being of special demand from the nuclear data community. In particular highly accurate data are needed for the new Generation-IV nuclear applications. The aim is to obtain precise neutron-induced fission cross-sections for ^{240}Pu and ^{242}Pu. In this context also accurate data on the spontaneous fission half-lives have been measured. To minimize the total uncertainties on the fission cross sections also the detector efficiency has been studied in detail. Both isotopes have been measured using a Twin Frisch-Grid Ionization Chamber (TFGIC) due to its superiority compared to other detector systems in view of radiation hardness, $2 \times 2\pi$ solid angle coverage and very good energy resolution. The present report summarizes the results so far achieved.

2.1 Introduction

In a recent assessment of target accuracies and uncertainties the OECD/Nuclear Energy Agency (NEA) highlighted the need for improved nuclear data to be used in model calculations for innovative reactor systems (GEN-IV) [8]. In this paper the neutron-induced fission cross sections of ^{240,242}Pu have been identified as of highest priority for fast neutron spectrum reactors. Their target uncertainties are very stringent and are requested to be 1-2% for ^{240}Pu and 3-5% for ^{242}Pu from current uncertainties of 6% and 20%, respectively.

In the frame of the ANDES collaboration (Accurate Nuclear Data for nuclear Energy Sustainability) several actinides are being under study, among them ^{240,242}Pu. Different experimental methods are being used to determine their neutron-induced fission cross section. For the first time the new digital data acquisition technique has been applied for cross section measurements. Using digital electronics and storing the full waveform opens up new analysis possibilities not available using regular analogue electronics.

The present report gives an overview of the present status of the experiment in terms of newly determined spontaneous fission half-lives for both ^{240,242}Pu and the resulting preliminary fission cross sections.

2.2 Experimental setup

A Twin Frisch-Grid Ionization Chamber (TFGIC) has been chosen as fission fragment (FF) detector. Its characteristics (radiation resistance, solid angle of nearly $2 \times 2\pi$ and good energy resolution) made this type of detector the excellent choice for performing direct kinematics fission experiments.

A schematic representation of the setup is presented in Fig. 2.1. Since the two samples used in this study have a thick backing, allowing to detect just one FF, they were placed in back-to-back geometry. The TFGIC was filled with P10 (90% Ar + 10% CH_4) as counting gas at a pressure of 1052 mbar with a constant flow of $\sim$ 50 ml/min. The cathode-grid distance was 31 mm and the grid-anode distance was 6 mm, allowing the FFs to be fully stopped within the space between the cathode and the grid. The cathode was common for the two samples and was set at a high voltage (HV) of -1.5 kV, while the two anodes were set at 1 kV. Both grids were grounded. Grids and anodes were connected to charge sensitive preamplifiers, and the output was fed into a 12 bit 100 MHz Waveform Digitizer (WFD). The cathode was connected to a current sensitive preamplifier. The output signal was split, one signal was fed into the WFD and the other was treated with a timing filter amplifier (TFA) and a constant fraction discriminator (CFD) resulting the trigger signal for all the WFDs.

The Pu samples used in this experiment were produced by the so-called *molecular plating* technique in the Target Preparation laboratory of the JRC-IRMM. Due to the short α half-life of the ^{240}Pu, 6561 yr (0.1%), the sample has a total mass of only 92.9 μg (0.4%) with an α-activity of 0.8 MBq (0.4%). The ^{242}Pu has an α half-life longer than 10^5 yr, for this reason more material could be deposited on top of the disk, being its mass of 671 μg (0.9%) and its α-activity of 0.1 MBq (0.3%). The main contribution on the mass uncertainty of ^{242}Pu is due to its α half-life and its uncertainty,

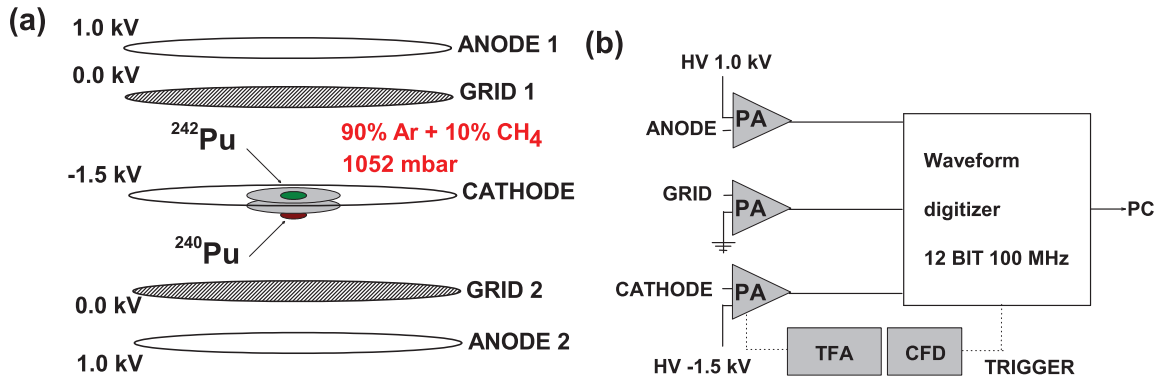

Figure 2.1: (a) Schematic drawing of a Twin-Frisch Grid Ionization Chamber (TFGIC) with the two samples inside. (b) Scheme of the electronics for one chamber side.

Table 2.1: Main characteristics of the ^{240,242}Pu samples [9]. All the uncertainties are expanded with a coverage factor $k = 1$. The expanded uncertainty of the sample purity has a coverage factor $k = 2$.

	^{240}Pu	^{242}Pu
Method	molecular plating	molecular plating
Chemical composition (assumed)	$Pu(OH)_4$	$Pu(OH)_4$
Total mass (μg) (calculated)	119.22 (0.4%)	859.54 (0.9%)
Total areal density (μg/cm^2) (calculated)	16.9 (0.4%)	122 (0.8%)
Backing	aluminium	aluminium
Mass (μg)	92.9 (0.4%)	671 (0.9%)
Areal density (μg/cm^2)	13.19 (0.4%)	95.3 (0.8%)
α-activity (MBq)	0.780 (0.4%)	0.0984 (0.3%)
Purity	99.8915(*18*)%	99.96518(*45*)%

3.75×10^5 yr (0.5%). The activity of both samples was determined by defined solid angle α-particle counting. The purity of the samples is higher than 99.8% and their atomic abundances were measured by mass spectrometry. The main characteristics of the ^{240,242}Pu samples are summarized in Tab. 2.1 [9].

The experiments were performed at the Van de Graaf (VdG) accelerator at IRMM. The neutron producing reactions used were ^{7}Li(p,n)^{7}Be and T(p,n)^{3}He giving the neutron energy range used in this study from 0.2 MeV to 3 MeV.

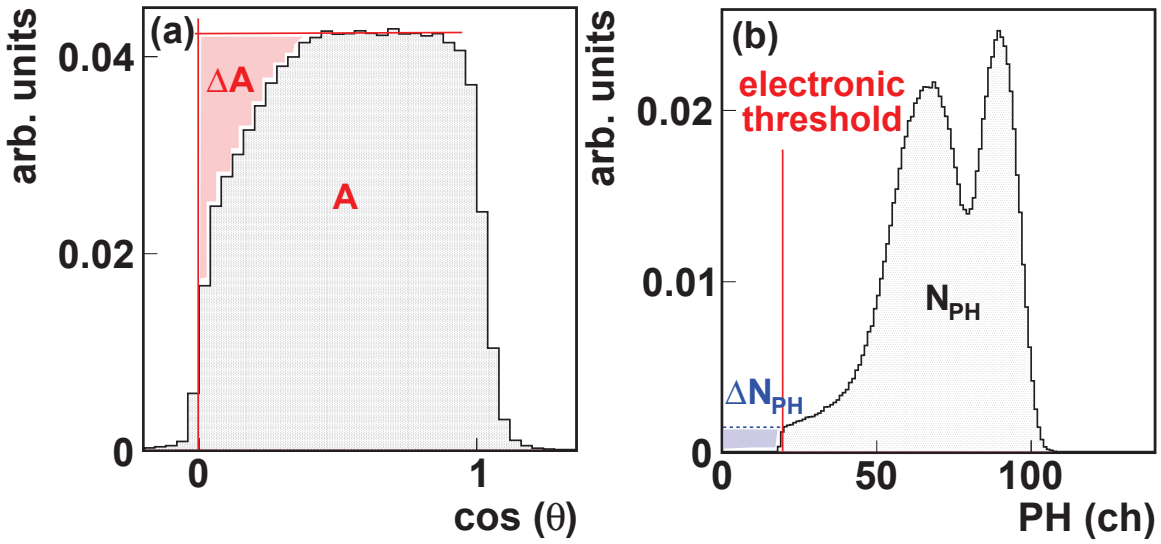

Figure 2.2: (a) Angular distribution for ^{242}Pu. The FF loss inside the sample is visible at low $\cos\theta$ values. By determining the integral of the distribution and ΔA (the missing part of the distribution) one can obtain the sample loss. (b) PH distribution for ^{242}Pu and determination of the counts under the electronic threshold.

2.3 Data analysis

Several corrections have been applied to the raw anode and grid signals. A detailed description is given in Ref. [10]. To determine the detection efficiency of the ionisation chamber the procedure as described in Ref. [11] has been used based on the following equation to determine the total number of emitted FFs (N_{cos}), one would do:

$$N_{cos} = A + \Delta A \tag{2.1}$$

with A being the integral of the cosine distribution and ΔA the missing part related with the thickness of the sample. To extract the sample loss it is needed to consider the anode PH distribution (N_{PH}) and extrapolate down to 0 (ΔN_{PH}) to account for FFs emitted but not detected due to the high electronic threshold requested not to trigger on α events (Fig. 2.2b). The experimental efficiency due to sample loss ($\epsilon_{\rm exp}$) will be calculated as:

$$\epsilon_{\rm exp} = \frac{N_{PH} + \Delta N_{PH}}{N_{cos}} = \frac{N_{2\pi}}{N_{cos}} \tag{2.2}$$

During the analysis of the P10 data we have found a strong correlation with the α-activity of the sample. Improving the signal risetime by using CH_4 as counting gas which has a twice higher drift velocity than P10 [12], the efficiency of the ionisation chamber also improved. To verify the

efficiency results obtained with the different analysis methods, theoretical calculations using SRIM [13] stopping power ranges and GEANT4 simulations [14] have been done.

The theoretical calculation has been done as presented in Ref. [11]. Properties for two typical FF have been used. The loss inside the sample can be calculated as:

$$\Delta_{\text{sample}} = \frac{t}{2R_{\text{sample}}} = \frac{t}{2}\sum_i \frac{W_i}{R_i} \tag{2.3}$$

with t as the thickness of the sample, R_i the range of isotope i and W_i the weight fraction of isotope i in the sample.

Simulations with GEANT4 have been performed with a FF kinetic energy distribution obtained with the GEF code [15]. From the simulations the transmitted FFs from the sample to the counting gas were obtained.

2.4 Spontaneous fission half-life

The SF half-life has been calculated using:

$$T_{1/2,SF} = \frac{\%^j\text{Pu}}{\text{A}_j}\frac{1}{\left(\frac{C_{SF}}{t\cdot\epsilon_j\cdot\ln 2\cdot m_{\text{Pu}}\cdot N_A} - \sum_i^n \frac{\%^i\text{Pu}}{\text{A}_i\cdot T_{1/2,SF}(i)}\right)} \tag{2.4}$$

where $\%^j$Pu is the purity of the sample, A_j its atomic mass, C_{SF} are the counts detected, ϵ_j is the detection efficiency, m_{Pu} is the sample mass, N_A the Avogadro's number and $\sum_i^n \frac{\%^i\text{Pu}}{\text{A}_i\cdot T_{1/2,SF}(i)}$ the contribution from the other isotopes contained in the sample.

Several measurements have been performed with each sample. Figure 2.3 summarizes in a graph the resulting $T_{1/2,SF}$ values. Run 1 for ^{240}Pu and 1-5 for ^{242}Pu were performed with P10 as counting gas, while runs 2-3 for ^{240}Pu and 6-7 for ^{242}Pu with CH_4. Each run contains several individual data sets with up to 250000 fission events using P10 and up to 150000 events using CH_4. All labelled runs are performed using a different electronic threshold. The error bars in the plot describe the statistical and the systematic uncertainties, the thick horizontal line is an eye guide for the weighted average of our data and the dotted lines are the final uncertainties (systematic and statistical) expressed with 1σ. The bullet symbols represent previous experimental results, the highlighted literature value is a weighted average of a subset of the literature data [16] and the Lit. Weight. Av. value is our weighted average of the same subset of data. In Tab. 2.2 the present uncertainty budget is listed and Tab. 2.3 lists the weighted average of our experimental data together with the weighted average of the literature values by Ref. [16] and the same weighted average calculated by us (Lit. Weight. Av.).

Our results are in agreement with the literature values for ^{242}Pu. Nevertheless, and using exactly the same method, the ^{240}Pu SF half-life is slightly higher than some of the literature values. This could be explained by the high α-activity of the sample. By having a more precise discrimination of α-particle signals our count rate might have been lower than in previous experiments done with analogue electronics, thus obtaining a higher SF half-life value. More details are given in Ref. [10].

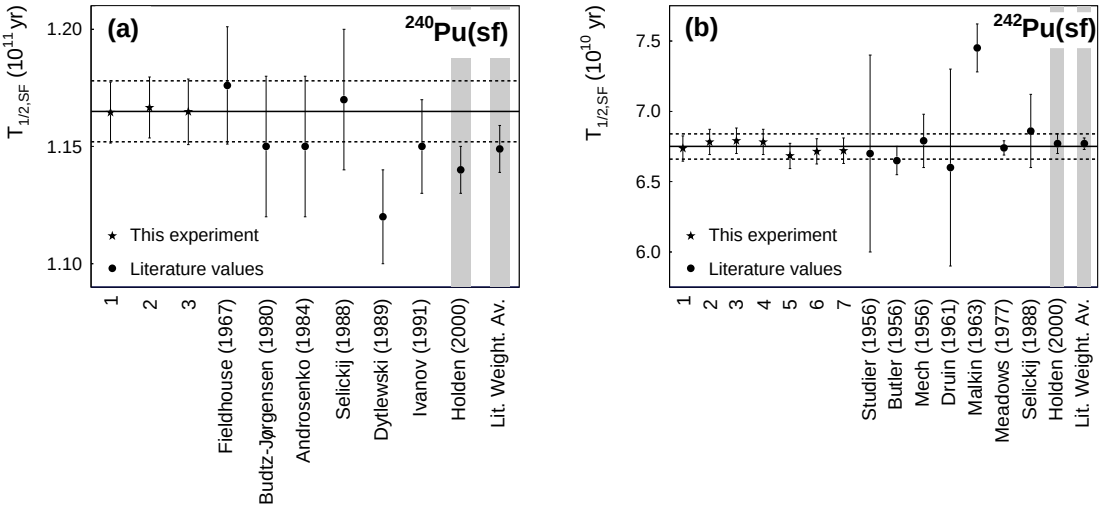

Figure 2.3: SF half-life results for ^{240}Pu (a) and ^{242}Pu (b) (stars) compared with some literature values (bullets), their weighted average calculated by Ref. [16] (Holden 2000) and the weighted average calculated by us using the data given by Ref. [16] (Lit. Weight. Av.). The thick line is the weighted average of all the experimental runs and the dotted lines are the total uncertainty on the weighted average. The mean was weighted with the statistical uncertainty and then adding the systematic component (1.1% for ^{240}Pu and 1.3% for ^{242}Pu). The literature values shown are the ones used by Ref. [16] to calculate the weighted average.

Table 2.2: Summary of the uncertainties corresponding to the SF half-life ($T_{1/2,SF}$) for ^{240,242}Pu.

Uncertainty source	^{240}Pu	^{242}Pu
Statistical	0.13%	<0.1%
Mass	0.4%	0.9%
Sample efficiency	1%	1%
Sample purity	<0.001%	<0.001%
Total (systematic and statistical)	1.1%	1.3%

2.5 Fission cross sections

The measurements have been performed at the Van de Graaff facility of the JRC-IRMM. Several campaings have been done for the two plutonium isotopes using the two different standards. The neutron producing reactions used were ^{7}LiF(p,n)^{7}Be for neutron energies between 0.2 MeV and 1.8 MeV and using ^{237}Np(n,f) as a reference cross section; and T(p,n)^{3}He for neutron energies between 1.8 and 3 MeV and using ^{238}U(n,f) as a reference. Based on the newly determined half-lives and efficiency

Table 2.3: Summary of the SF half-life ($T_{1/2,SF}$) for ^{240,242}Pu. The experimental uncertainties presented are both the statistical and systematic. The weighted average of literature values presented by Ref. [16] and the one calculated by us (Lit. weighted Av.) using the same data as Ref. [16] are given as well.

$T_{1/2,SF}$ (yr)	^{240}Pu	^{242}Pu
Holden (2000) [16]	$1.14 \times 10^{11}(0.9\%)$	$6.77 \times 10^{10}(1.0\%)$
Lit. weighted Av.	$1.15 \times 10^{11}(0.9\%)$	$6.77 \times 10^{10}(0.6\%)$
This experiment	$1.165 \times 10^{11}(1.1\%)$	$6.75 \times 10^{10}(1.3\%)$

determination of the ionisation chamber the fission cross sections have been calculated for both ^{240}Pu and ^{242}Pu according to the following equation:

$$\sigma_{\mathrm{Pu}}(E_n) = \left[\frac{N_{\mathrm{ref}}}{N_{\mathrm{Pu}}} \cdot \frac{(\frac{C_{\mathrm{Pu}}}{\epsilon_{\mathrm{Pu}}} - C_{\mathrm{SF}})}{\frac{C_{\mathrm{ref}}}{\epsilon_{\mathrm{ref}}}} - \sum_i P_i \cdot \frac{\sigma_i(E_n)}{\sigma_{\mathrm{ref}}(E_n)} \right] \cdot \sigma_{\mathrm{ref}}(E_n) \tag{2.5}$$

where N_i are the number of atoms in the sample i, C_i are the number of counts detected from the sample i, C_{SF} are the number of spontaneous fission counts from the plutonium sample, ϵ_i is the transmission probability of a fission fragment (FF) to leave the sample and enter into the counting gas, $\sum_i P_i \cdot \frac{\sigma_i(E_n)}{\sigma_{\mathrm{ref}}(E_n)}$ is the contribution on the plutonium fission counts from the impurities of the sample and $\sigma_{\mathrm{ref}}(E_n)$ is the cross section from the reference isotope. The uncertainty calculation includes the contribution of the sample mass, the uncertainties on the half-life and isotope content, statistics and efficiency.

The result is given in Fig. 2.4, to the left side for ^{240}Pu and the right side for ^{242}Pu, respectively.

Two different normalizations have been performed. At first, the data were normalized to the ENDF/B.VII.1 evaluation [17] for the two reference isotopes (^{237}Np - blue symbols- and ^{238}U - red symbols-). A clear discrepancy between the data relative to the ^{237}Np evaluation and the ^{238}U evaluation is observed. The difference at the overlapping incident neutron energy points amounts to about 13% in both cases. The data for both ^{240}Pu and ^{242}Pu measured relative to the ^{238}U fission cross section agree very well with the JEFF 3.1 evaluation. The threshold for ^{240}Pu is very well reproduced and also agrees best with the JEFF 3.1 evaluation. There is a distinct difference above threshold for both Pu isotopes if the ^{237}Np ENDF/B-VII.1 evaluation is used.

Recently, new values for the neutron-induced fission cross section for ^{237}Np were published by [18], these data were around 5% higher in value than the current evaluations (see Fig. 2.5). By normalizing our ^{237}Np data to Ref. [18], the green symbols would be obtained in Fig. 2.6. Then in case of ^{240}Pu the new results would be much better in agreement with the ENDF/B-VII.1 evaluation over the whole energy range covered by the ^{237}Np reference. For ^{242}Pu however, both the threshold and above threshold values are still too small compared to the ENDF/B-VII.1 evaluation. The difference in the overlap region to the ^{238}U reference data is in both cases still 5-8%.

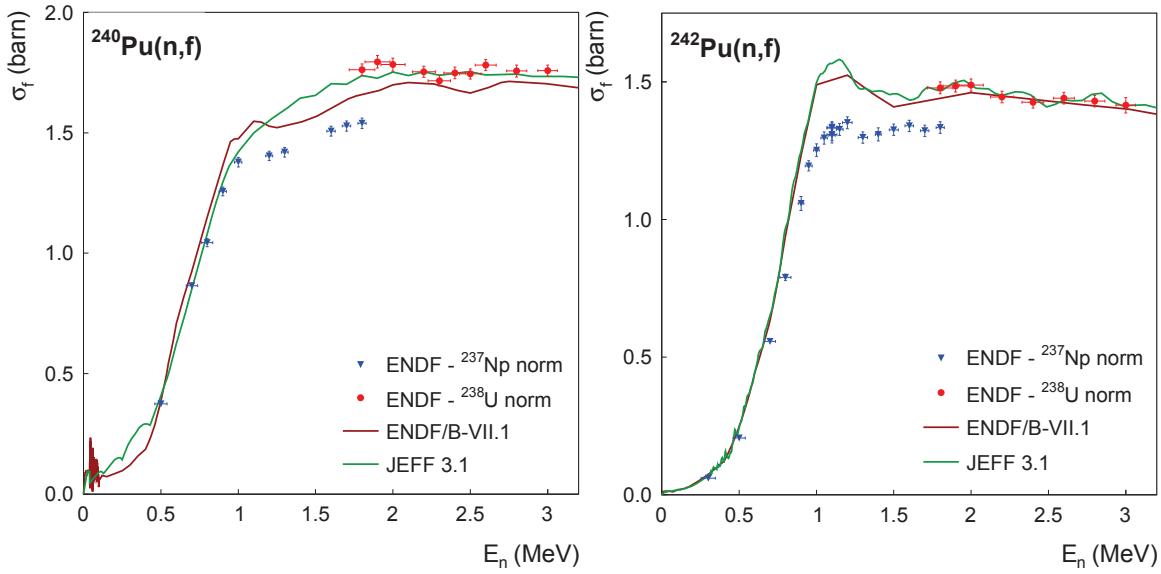

Figure 2.4: Neutron-induced fission cross section of ^{240}Pu (left) and ^{242}Pu (right). The triangles represents our data taken relative to the ENDF/B-VII.1 ^{237}Np evaluation; while the bullets is data taken relative to the ENDF/B-VII.1 ^{238}U evaluation.

2.6 Conclusions

The neutron-induced fission cross section has been measured for ^{240,242}Pu at the Van de Graaff facility of the JRC-IRMM. The energy range studied has been between 0.2 MeV and 3 MeV neutron incoming energy. Two different secondary standards have been used: ^{237}Np and ^{238}U. The results obtained at the overlap neutron energy region for the two standards used (1.8 MeV) do not agree within uncertainties. The preliminary results presented in Fig. 2.4 do neither agree with each other nor with evaluations. All points to a too small ^{237}Np fission cross section. New measurement of this cross section by Paradela et al. [18] are 5% larger compared to the present evaluation but are still too small to make the match in the overlap region between the two standards.

Acknowledgments

One of the authors (P.S.-C.) aknowledges financial support from the ANDES collaboration (contract FP7 - 249671).

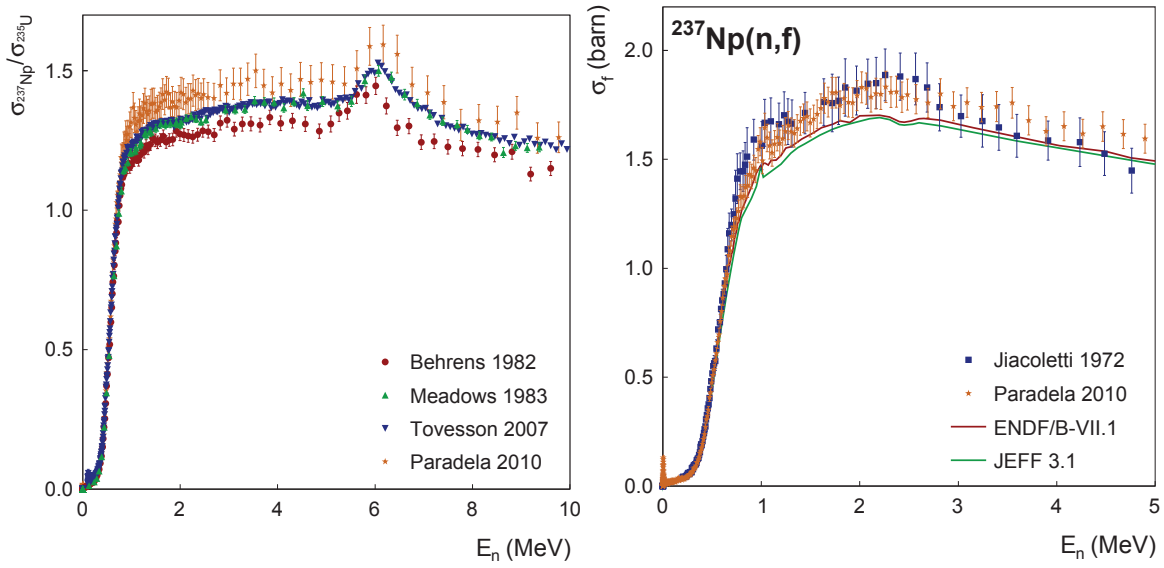

Figure 2.5: Left: ratio of the neutron-induced fission cross section of ^{237}Np and the ^{235}U. Three groups of data are distinguished. Right: neutron-induced fission cross section fof ^{237}Np; the latest evaluations are shown together with data from Ref. [18, 19].

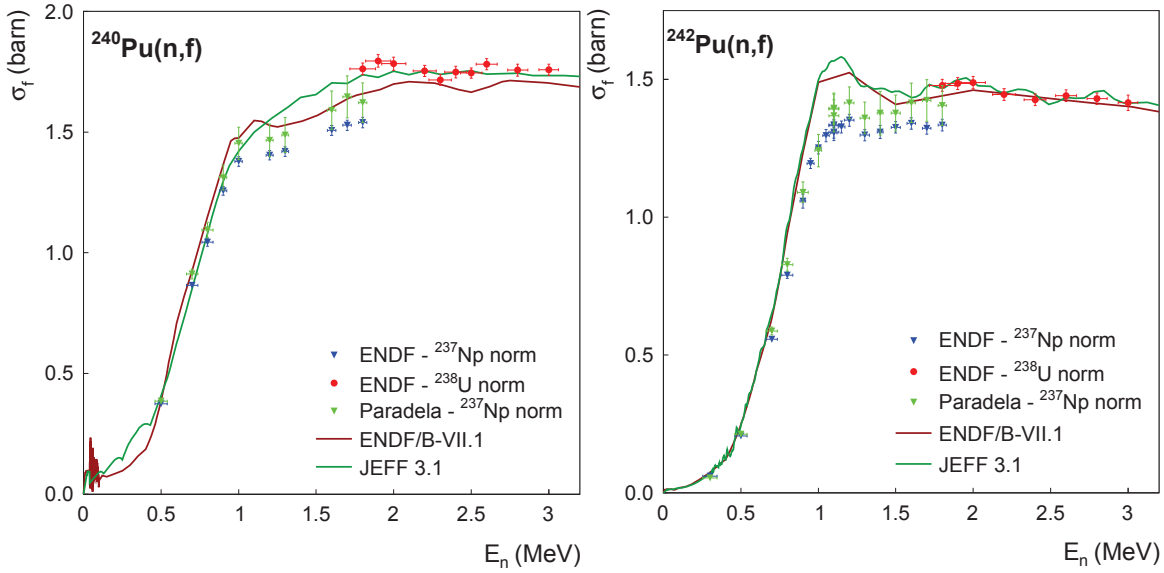

Figure 2.6: Neutron-induced fission cross section of ^{240}Pu (left) and ^{242}Pu (right). The blue triangles represents our data taken relative to the ENDF/B-VII.1 ^{237}Np evaluation; while the bullets is data taken relative to the ENDF/B-VII.1 ^{238}U evaluation. A new normalization of the ^{237}Np data is presented relative to the new cross sections values of Ref. [18].

Chapter 3

Measurement of the ^{240,242}Pu(n,f) cross section at the CERN n_TOF facility

A. Tsinganis[1,21], E. Berthoumieux[3], C. Guerrero[2], N. Colonna[4], M. Calviani[2], R. Vlastou[1], S. Andriamonje[2], V. Vlachoudis[2], F. Gunsing[3], C. Massimi[5], the n_TOF Collaboration

1) National Technical University of Athens (NTUA), Greece

2) European Organisation for Nuclear Research (CERN), Geneva, Switzerland

3) Commissariat à l'Énergie Atomique (CEA) Saclay - Irfu, Gif-sur-Yvette, France

4) Istituto Nazionale di Fisica Nucleare, Bari, Italy

5) Dipartimento di Fisica e Astronomia, Universita' di Bologna, and Sezione INFN di Bologna, Italy

6) www.cern.ch/ntof

3.1 Experimental setup

3.1.1 The n_TOF facility

The ^{240,242}Pu(n,f) cross sections are included in the NEA High-Priority List [6] and were measured at the CERN n_TOF facility [20, 21, 22] relative to the well-known ^{235}U(n,f) cross section. At n_TOF, neutrons are produced through spallation induced by a 20 GeV/c bunched proton beam impinging on a massive lead target and subsequent moderation in a few centimetres thick layer of (borated) water. The produced neutrons have energies starting from thermal and up to over 10 GeV and travel

[1]E-mail: Andrea.Tsinganis@cern.ch

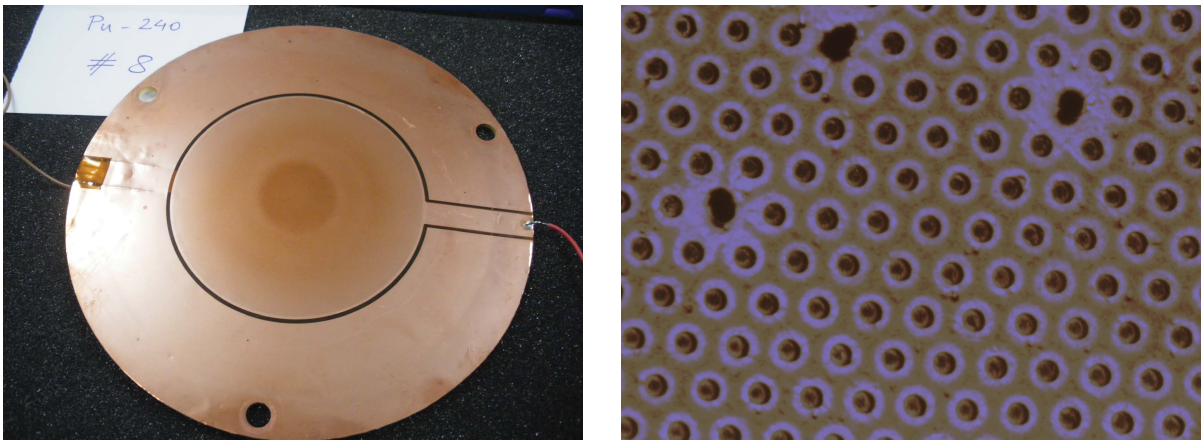

Figure 3.1: Left: One of the Micromegas detectors used with a ^{240}Pu sample pictured after the end of the measurement. A 3 cm diameter discolouration is visible on the micromesh. Right: Picture of the micromesh taken with an electronic microscope. Mechanical damage around the rims of the holes can be observed. This leads to a severe deterioration of the detector gain and performance.

along an approximately 185 m long path to reach the experimental area. This allows to cover the region of interest in a single experiment, thus reducing uncertainties related to different measurements performed in separate neutron energy ranges. The high instantaneous flux of the n_TOF neutron beam mitigates the adverse effects of the strong α-particle background produced by the samples and the low fission cross section below and near the fission threshold.

3.1.2 Samples

Eight plutonium oxide (PuO_2) samples manufactured at IRMM, Geel, were used **(author?)** [23] ($4\times^{240}PuO_2$, $4\times^{242}PuO_2$), for a total mass of 3.1 mg of ^{240}Pu (~0.11 mg/cm^2 per sample, 99.90% purity) and 3.6 mg of ^{242}Pu (~0.13 mg/cm^2 per sample, 99.97% purity). The material was electro-deposited on an aluminium backing 0.25 mm thick and 5 cm in diameter, while the deposit itself had a diameter of 3 cm. Various contaminants were present, mainly in the form of other plutonium isotopes, such as ^{238}Pu, ^{239}Pu, ^{241}Pu and ^{244}Pu. While these impurities are present in very small amounts, the high fission cross sections of fissile contaminants compared to the isotopes of interest dominate in parts of the energy range studied.

Additionally, a ^{235}U sample (UF_4) with a mass of 18 mg deposited on a 0.2 mm thick aluminium backing was used as reference. Since this sample had a diameter of 7 cm, its active area was reduced with a thin aluminium mask to match the diameter of the plutonium samples. The active mass was therefore reduced to 3.3 mg of ^{235}U (~0.47 mg/cm^2).

3.1.3 Detectors and data acquisition

The measurements were carried out with Micromegas (Micro-MEsh GAseous Structure) gas detectors [24]. The gas volume of the Micromegas is separated into a charge collection region (several mm) and an amplification region (typically tens of μm) by a thin "micromesh" with 35 μm diameter holes on its surface. The amplification that takes place in the amplification region significantly improves the signal-to-noise ratio of the detector. This is of special importance for the high neutron energy region, where the fission signals are recorded within a few μs of the γ-flash (see section 3.2.2). A chamber capable of holding up to 10 sample-detector modules was constructed and used to house the plutonium and uranium samples. The chamber was filled with an Ar:CF_4:isoC_4H_{10} gas mixture (88:10:2) at a pressure of 1 bar and under constant circulation.

Existing electronics from previous fission measurements were used for signal shaping. Additional electronic protection was added to the pre-amplifier channels to prevent breakage, while the mesh voltage value was chosen to minimize the number of sparks and subsequent trips. Furthermore, the shielding of the pre-amplifier module was improved to mitigate the baseline oscillation observed following the prompt γ-flash. The standard n_TOF Data Acquisition System [20] based on 8-bit Acqiris flash-ADCs was used for recording and storing the raw data collected by the detectors at a sampling rate of 100 MHz.

Due to the low expected count rate for the measurement, the chamber was placed in the n_TOF experimental area for several months and in parallel with other measurements performed at n_TOF. Throughout the measurement, beam-off data were taken in order to record the α- and spontaneous fission background produced by the samples.

3.1.4 Experimental issues

The analysis of the experimental data is complicated by certain features of the experimental setup and by sample-induced backgrounds. These include the baseline oscillation induced by the prompt "γ-flash" which is discussed in section 3.2.2 and the spontaneous fission background, particularly in ^{242}Pu.

While the above factors can be dealt with, an unexpected effect of the high α-activity of the samples (>6 MBq for ^{240}Pu) was encountered. After the end of the measurement, a visual inspection of the detectors used with the ^{240}Pu samples revealed a remarkable feature. As seen in fig. 3.1 (left panel), an obvious circular discolouration of the mesh whose dimension and position exactly matched those of the samples was observed. Upon closer inspection with a microscope (fig. 3.1, right panel), it became clear that the micromesh had suffered serious mechanical damage, particularly around the rims of the holes which were evidently deformed.

The mechanical damage suffered by the detectors must lead to a deterioration of the electrical field and therefore of the detector gain and overall performance. Indeed, this was clearly observed in the ^{240}Pu data, where fission fragment and α-particle signals became virtually indistinguishable in the obtained pulse height spectra. Because of this, a considerable part of the ^{240}Pu data must be discarded, partially compromising the measurement. Although there was no visible damage, a similar

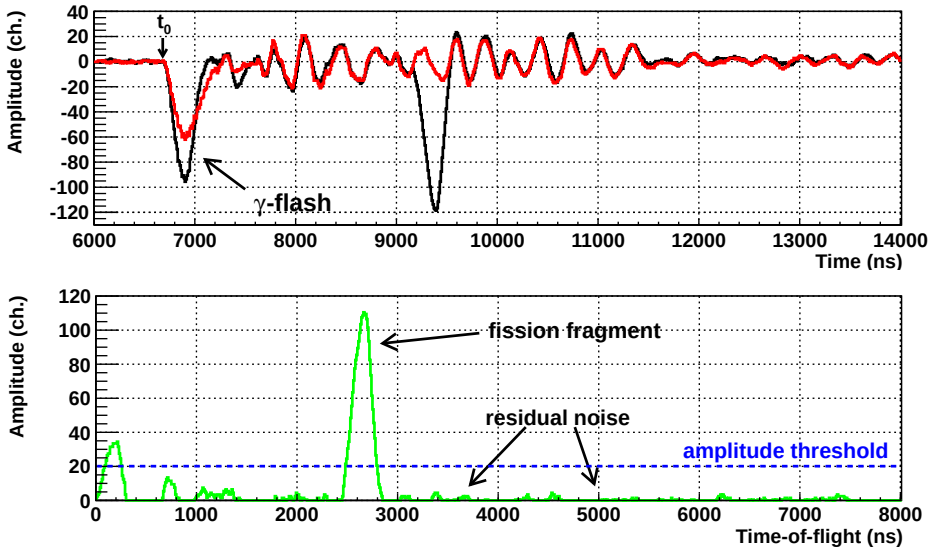

Figure 3.2: Top panel: The beginning (first few μs) of the recorded signals during the same proton bunch from two adjacent detectors. The γ-flash signal and the baseline oscillations are clearly visible. Bottom panel: the residual signal after the subtraction of the two signals above. The oscillation is almost entirely suppressed.

but less pronounced effect was observed in the ^{242}Pu data, in the form of a slow but non-negligible gain shift throughout the duration of the measurement. The data, therefore, need to be analysed in smaller subsets where the gain can be considered constant.

For the above reasons, preliminary results on ^{242}Pu only are being presented in this report.

3.2 Analysis and results

3.2.1 Raw data analysis

The raw data from each detector are analysed by means of a pulse recognition routine that determines the amplitude and position in time of the detected signals, among other quantities. The signal baseline is determined by analysing the pre-trigger and post-acquisition window data, accounting for possible signals (α or spontaneous fission) that may be present. Since the Pu samples are in the same chamber as the ^{235}U it can be assumed that they receive the same neutron flux, while the fission count rates are sufficiently low to ignore pile-up effects.

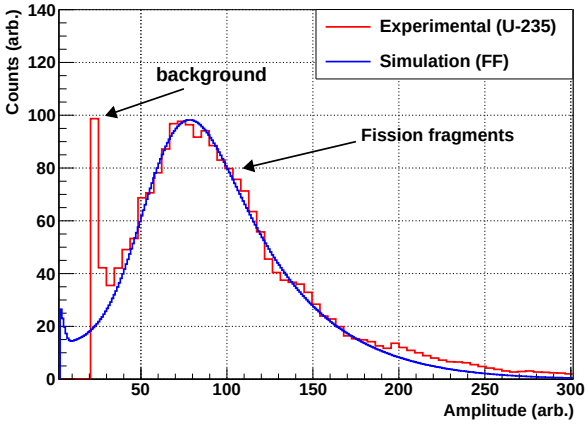

Figure 3.3: Experimental (red) and simulated (blue) pulse height spectra for ^{235}U. The cut-off of the low-amplitude signals is due to the threshold set in the peak-search routine.

3.2.2 The high neutron energy region

The interactions of the proton beam with the spallation target lead to a significant production of prompt γ-rays and other relativistic particles that reach the experimental area at (nearly) the speed of light and constitute the bulk of what is commonly termed the "γ-flash". In Micromegas detectors, this causes an initial signal lasting a few hundred ns, followed by a baseline oscillation that lasts for several μs or, in terms of neutron energy, down to 1-2 MeV. This behaviour can be observed in fig. 3.2 (top panel), where the baseline oscillations are clearly visible.

This problem can be mitigated by applying a software "compensation" technique [25] to the digitally recorded data. This method is based on the observation that the oscillations recorded in adjacent detectors for the same proton bunch are almost identical. This can be seen by comparing the recorded signals from two detectors placed consecutively in the chamber (fig. 3.2, top panel). The subtraction of the output of adjacent detectors causes the oscillations to largely cancel each other out, leaving a residual signal that consists primarily of signals attributable either to fission fragments or α-particles (fig. 3.2, bottom panel). This signal is then analysed with the peak search routine used for the lower energy region, thus extracting the desired pulse height spectra. The small residual of electronic noise is generally well below the amplitude threshold for fission fragment detection.

3.2.3 Monte-Carlo simulations

The behaviour of the detectors was studied by means of Monte Carlo simulations performed with the FLUKA code [26, 27], focusing particularly on the reproduction of the pulse height spectra of α-particles and fission fragments for the evaluation of the detector efficiency and the quality of the peak-search routine. In fig. 3.3, an experimental pulse height spectrum obtained from ^{235}U and a simulated fission fragment spectrum can be compared.

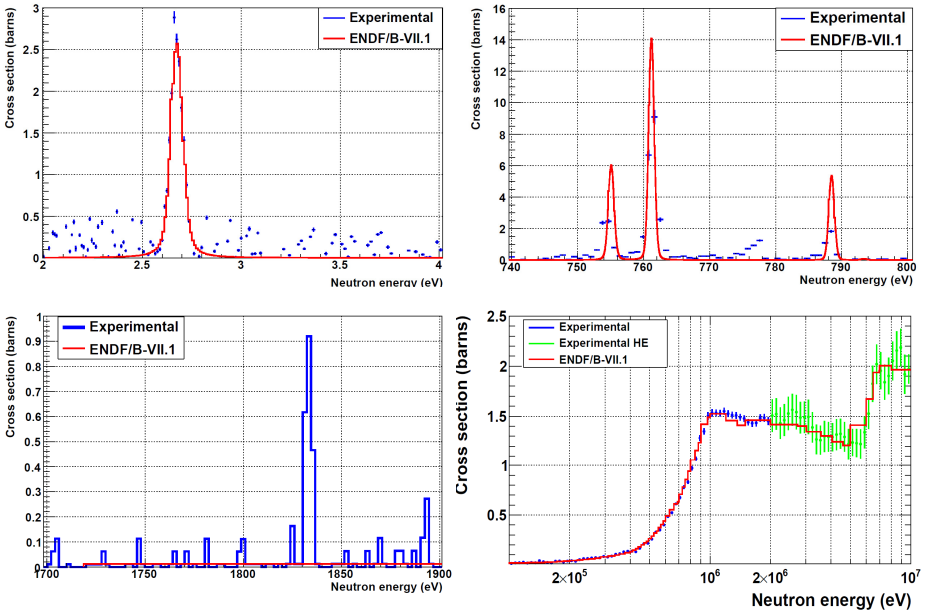

Figure 3.4: The first ^{242}Pu resonance at 2.7 eV (top left panel) and resolved resonances between 750 and 800 eV (top right) and around 1800 eV (bottom left). Data above the fission threshold (bottom right). Above 2 MeV, data are treated with the method described in section 3.2.2. The use of this CPU-intensive method means only a subset of the available statistics has been processed, hence the larger uncertainties pictured here.

3.2.4 Present results

The spontaneous fission background dominates the low energy region and remains visible up to about 10 keV. Still, several resonances can be observed above this background. The first ^{242}Pu resonance at ~2.7 eV can be seen in the top left panel of Fig. 3.4, after subtraction of the spontaneous fission background, as determined with a fit of the beam-off data. The top right and bottom left panels panel show resolved resonances in the 700-800 eV region and up to approximately 1900 eV, including one at ~780 eV and one at 1830 eV not present in the evaluated libraries and, at a preliminary analysis, not attributable to any of the stated sample impurities. Additional resonance candidates at higher energies have been observed. Data above 1 keV are shown in the bottom right panel of Fig. 3.4. The data displayed are combined from the two analysis methods; the conventional "straightforward" analysis, which fails above about 2 MeV due to the baseline oscillations, and the high-energy analysis described in section 3.2.2. The analysis of the high energy region will be extended up to about 100 MeV.

3.3 Conclusions

3.3.1 Status of the analysis

Preliminary results from the ^{242}Pu(n,f) experiment performed at the CERN n_TOF facility are presented. The experimental setup and analysis method is described, including auxiliary Monte-Carlo simulations and an off-line technique to recover high-neutron energy data affected by the prompt γ-flash.

Analysis of the ^{242}Pu(n,f) data is well under way and is only complicated by the gradual detector gain shift. Among the issues still to be addressed are the exact determination of the detector efficiency and the amplitude threshold correction, the accurate subtraction of the spontaneous fission background and the estimation of all uncertainties involved. The analysis of the high-energy region data is particularly CPU-intensive and is therefore proceeding at a relatively slow pace, given the amount of data acquired during the measurement.

Finally, a significant part of the ^{240}Pu(n,f) was discarded due to the damage suffered by the detectors, as explained in section 3.1.4. Even under normal detector operation, the high α-pileup probability (>30%) produces a long tail in the amplitude spectra that adversely affects the α - fission fragment separation. In order not to set a very high amplitude threshold that would further reduce the statistics, an alternative approach – characterising and subtracting the α-background – will be employed.

3.3.2 Publications

To this date, two conference proceedings have been submitted, to the Nuclear Data Conference (New York, March 2013) and to the International Nuclear Physics Conference (Florence, June 2013). Both are expected to be published in the first half of 2014. Once the analysis is terminated, a dedicated paper will be submitted to a peer-reviewed journal.

Chapter 4

Measurement of the fission cross section of ^{240,242}Pu relative to the standard ^{1}H(n,p) at CENBG

M. Aiche[1], L. Mathieu[1], G. Kessedjian[2], P. Salvador[3,4], A. Plompen[3], B. Jurado[1], S. Czajkowski[1], J. Mattaranz[1], Q. Ducasse[1], 5, G. Beliet[6], G. Boutoux[6], J. Taieb[6]

1) CENBG-IN2P3-CNRS, BP120, 33175 Gradignan, France.

2) LPSC-IN2P3-CNRS, 53 Avenue des Martyrs, 38026 Grenoble, France.

3) European commission, Joint Research Centre, Institute for Reference Materials and Measurements (JRC-IRMM), Retieseweg 111, B-2440 Geel, Belgium.

4) Institute of Energy Technologies, Technical University of Catalonia, Avda. Diagonal 647, E-08028 Barcelona, Spain.

5) CEA, DEN, DER, F-13108 Saint Paul Lez Durance, France.

6) CEA-DAM, SPhN, 91680 Bruyères-le-Châtel, France.

Abstract

The existing evaluations of the ^{240,242}Pu neutron-induced fission cross section have been questioned by recent sensitivity studies. In the neutron energy range from 0.5 to 2.2 MeV and 0.5 to 6 MeV for ^{240}Pu and ^{242}Pu respectively, where the current uncertainties are scattering from 6% to 20%, for ^{240}Pu and 20%, for ^{242}Pu, they should be reduced to the desired accuracy request at a level which is less than 5%.

To achieve this goal we have used the neutron-proton scattering cross section as reference reaction in order to determine the incident neutron flux. This cross section is known with a precision better than 1 % for a wide range of neutron energies (1 meV to 20 MeV). A first experiment has been performed at the 4MV Van-de-Graaff accelerator of the BRC-CEA-DIF (Bruyères-le-Châtel), in the neutron energy range from 1.1 to 2.0 MeV. The neutrons were produced via the T(p,n)^{3}He reaction using a solid TiT target of 952 μg/cm^2 impinged by a proton beam of 1.9, 2.3 and 2.8 MeV with an average intensity of 4.5 μA. In order to achieve the required measurements, we have performed a first quasi-absolute measurement of these fission cross sections in the plateau region. The data analysis showed that the fission detector is very sensitive to the alpha radioactivity of the samples. The solar cells used as fission detector have been seriously damaged with the alpha radioactivity of the ^{240}Pu sample. The recorded data of the present experiment do not allow us to determine the fission cross section for ^{242}Pu due to a malfunction of the SCALER module of the acquisition system.

However, we are optimistic to obtain the fission cross section of ^{242}Pu at 2.0 MeV neutron energy. A simulation of the entire experimental setup is needed in order to reproduce the observed recoil protons spectrum and then to infer the neutron flux impinging on the ^{242}Pu sample.

4.1 Introduction

Recent sensitivity analysis studies [4,6,28] have been performed for different types of advanced nuclear systems, in particular for Generation-IV fast reactors. These studies indicate that an important reduction of the uncertainties on nuclear data is needed for many actinides, such as fission cross-section for both ^{240}Pu and ^{242}Pu isotopes in the fast neutron region.

The ^{240}Pu and ^{242}Pu are produced in the nuclear fuel during the nuclear fission process of thermal or fast reactors by successive neutron captures and α or β decays. Both isotopes are particularly unsuited for recycling in a thermal reactor, due to their non-fissile property and low fission cross-section. Indeed, their relatively long half life ($T_{1/2}$(^{240}Pu) = 6561 y and $T_{1/2}$(^{242}Pu) = 3.75x10^5 y) favors the neutron capture reaction where heavier nuclei are typically produced faster than ^{240}Pu and ^{242}Pu are transmuted. A more efficient burning via the fission process would occur in a fast reactor, where the harder fission neutron spectrum would better match the fission threshold of both isotopes. The first assessment of the nuclear data needs has been performed in Ref. [4]. This study has indicated the desired accuracy on nuclear data, for different types of new generation reactors that should be reached in order to meet the requirements on integral parameters of those systems [6].

More specifically, sensitivity studies (Ref. [4] and [6]) show that ^{240}Pu and ^{242}Pu are among the highest priority isotopes for which the accuracy has to be increased. In particular the data have to be improved in the region between 0.5 and 2 MeV for the ^{240}Pu(n; f) reaction, where the current uncertainties, scattering from 6% to 20%, should be reduced to the level less than 5%. For the ^{242}Pu(n,f) reaction, for the cross section in the region from 0.2 to 6 MeV, currently known to the precision of ~20%, the desired accuracy request is put close to 3-5%.

The present work aimed at collecting new data on neutron-induced fission cross-section for ^{240}Pu and ^{242}Pu in the energy range from 1.1 MeV to 2.0 MeV, in reference to the neutron-proton (n,p) elastic scattering cross section, which is known with a precision better than 0.5%, over a wide neutron-energy range of 1 MeV to 20 MeV [29]. The target accuracy should be better than 4-5%. The chosen region of energies covers the beginning of the plateau, i.e. exactly the regions which are important for the new generation reactor applications and where the accuracy on the nuclear data should be improved.

The ^{240}Pu(n,f) reaction has been studied in the 50's and early 60's, mainly in the context of fast nuclear reactor development. Several measurements have been performed from the threshold region up to some tens of MeV starting from the 70s. In this energy range the available data generally agree between themselves within the experimental uncertainties but in some local regions the disagreement is up to 6%. However, since most of these data refer to the same normalization point, their relevance is strongly reduced. Recent measurements [30,31] extended the measurement up to 200 MeV, finding comparable results with very low statistical uncertainties.

For ^{242}Pu the situation of the existing experimental data is worse in the threshold region where the discrepancies between various results are up to 15%. Various other experimental data are available for the region from the onset of the fission threshold up to few MeV, with discrepancies higher than 10-15%.

4.2 Experimental setup

The neutron-induced fission cross section measurements campaign for ^{240}Pu and ^{242}Pu have been performed at the 4MV Van-de-Graaff accelerator of the BRC-CEA-DIF (Bruyères-le-Châtel), in december 2012, in the neutron energy range from 1.1 to 2.0 MeV. The neutrons were produced via the T(p,n)^{3}He reaction using a solid TiT target of 952 µg/cm² impinged by a proton beam of 1.9, 2.3 and 2.8 MeV with an average intensity of 4.5 µA. The experimental set-up used during the measurements campaign is illustrated here after in ***Fig. 1***.

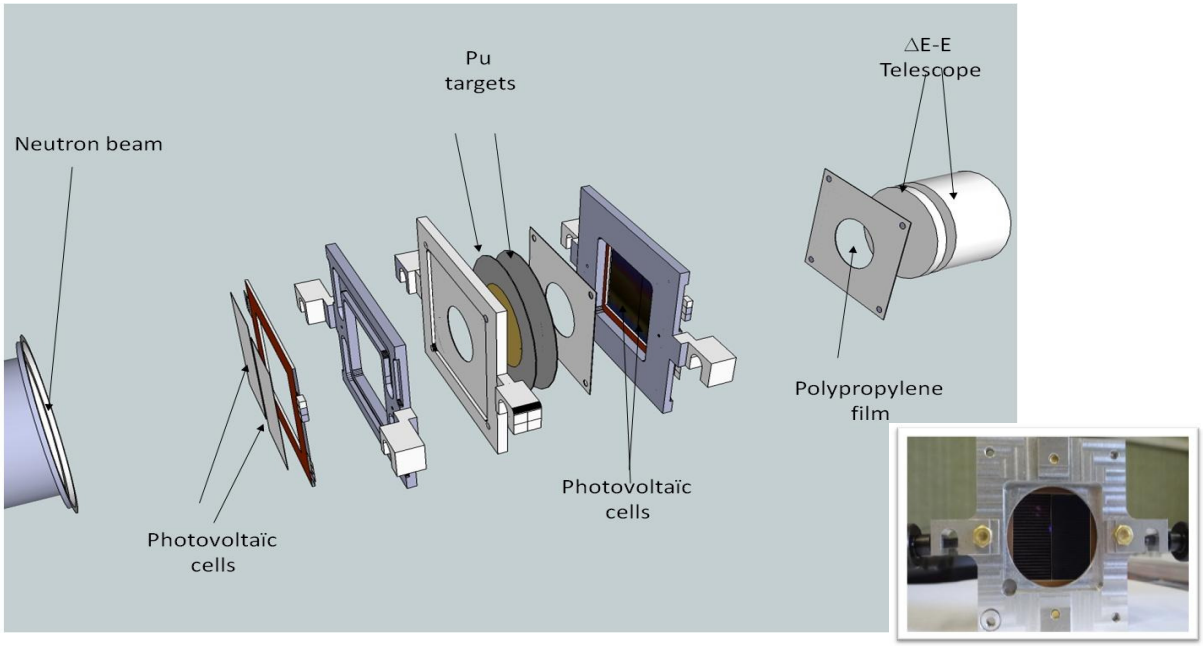

Figure 1 Exploded view of the experimental setup showing at foreground the fission fragment detector. The neutron beam passes through the Pu samples and the Polypropylene film.

The two samples of ^{240}Pu and ^{242}Pu were placed back to back in a vacuum chamber at 54.7 mm from the neutron source and at 0° with respect to the incident neutron beam. Each layer (diameter 28 mm) was prepared at the IRMM by electroplating techniques onto a 0.25 mm thick Aluminum backing; the samples thicknesses are about 260 µg/cm^2 with an alpha radioactivity of 0.23 MBq for ^{242}Pu and 13.2 MBq for ^{240}Pu. The fission detector which consists of two sets of photovoltaic (solar) cells [32] were placed in front of each Pu isotope layer in a very compact geometry at a distance of 5.3 mm to obtain a geometrical efficiency of around 72%. A complete separation between alpha particles and fission fragments [32,33] is one of the strengths of the detector. However, the detector is able to achieve this performance, provided that the alpha radioactivity remains low. The photovoltaic cells have also no sensitivity to the neutron beam and their intrinsic efficiency is of 95±1 %.

The neutron flux measurements were performed with a proton-recoil detection system. It consist of a polypropylene (PP) foil of different thicknesses ($(C_3H_6)_n$) and a silicon E or ΔE-E Telescope depending on the neutron energy range, see ***Fig. 1***. The PP foil (diameter of 15 mm) is placed at 89.7 mm from the neutron source and at 0° with respect to the incident neutron beam. Recoiling protons emitted at forward angles by the neutron-proton elastic scattering reaction occurring in the PP foil, are detected with a silicon detector E placed at 78.8 mm from the PP foil, having a thicknesses of 300 µm. A PP foil of 4 µm was chosen to cover the 1.1 to 2 MeV neutron energy range. The maximum energy loss for the recoiling protons was kept below 10% [34]. The main concern of this

experiment is to perform a background subtraction of the detected protons generated by neutrons scattered from the detectors, samples or other materials close to the Silicon E detector. The recoiling proton spectrum was measured at each energy with two separate measurements, namely, a standard measurement followed by a background measurement. For the standard measurement, the Telescope is in front of the polypropylene (PP) foil. For the background measurement, the recoiling protons are stopped in a removable tantalum screen placed between the PP foil and the Silicon detector. The tantalum thickness is adapted to stop the highest energy protons**.** The spectrum that results from the background subtraction should present only one peak corresponding to the protons produced by the interaction of the quasi-monoenergetic incident neutrons with the PP foil.

A He_3 and BF_3 neutron monitors placed respectively at 0 and 30 degree with respect to the incident-neutron beam were used in order to normalize the standard and background measurements of the recoil protons at same neutron energy.

4.3 Data Analysis

In principle, the neutron flux on the PP foil is obtained by integrating the measured recoiling protons spectrum combined to the well known n-p elastic cross section together with the Silicon E detector efficiency. By computing the ratio of the solid angles subtended by the targets and the PP foil, we infer then, the neutron flux on the Pu deposits. However, the neutron spectrum at the PP-foil is not stricly monoenergetic and one has to consider an average n-p cross section. Moreover, it is not obvious how to determine precisely the Silicon E detector efficiency in an analytical way. For this reason, Monte-Carlo simulations for neutrons and protons passing through the experimental setup are necessary. The simulation code will allow us to determine the neutron energy spectrum impinging the ^{240,242}Pu targets or the PP foil, taking into account the resolution of the charged particle beam, the energy loss of the charged particle beam in the tritium target, the angular distributions of the neutron beam, the angular distribution of the (n,p) elastic scattering cross sections [29], the proton energy loss in the PP foil and the energy resolution of the Si Telescope detectors.

The kinematic effects and the uncertainties on geometrical parameters will be taken into account to define precisely the value and the precision of the fission-fragment detection efficiency, which is one of the most important sources of uncertainty in this experiment. The large angular acceptance of fission detectors involves low sensitivity to the fission-fragment angular anisotropy.

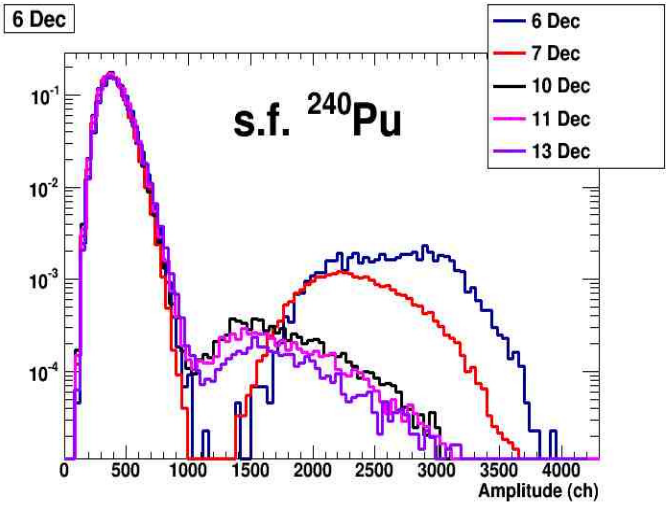

Figure 2 Time evolution of the alpha pile up and spontaneous fission spectra of the ^{240}Pu sample.

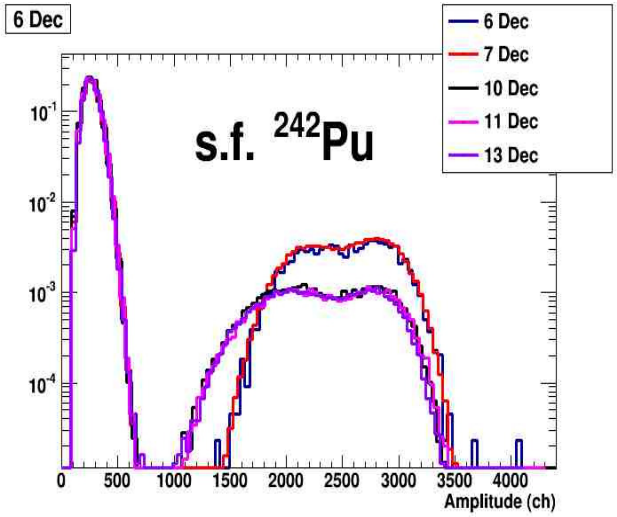

Figure 3 Time evolution of the alpha pile up and spontaneous fission spectra of the ^{242}Pu sample.

The proposed experiment aims to minimize the statistical and experimental uncertainties.

We started the analysis by a systematic verification of the consistency of the collected data. The first observation concerns the fission detector as shown in the figure 2, is sensitive to alpha decay of the Pu samples.

The observed degradation of the photovoltaic cells associated to the fission fragments detector for the ^{240}Pu sample is changing rapidly at the beginning of the measurements campaign (6, 7 and 10 december) before reaching a certain limit. In the figure 3, the solar cells of the fission detector dedicated to the ^{242}Pu sample, are more resistant to the alpha radioactivity. The observed difference in the fission fragments distribution is due to the electronic threshold which was much higher for the spectrum of 6 and 7 december compared to the spectrum beyond 10 December.

Finally, we have made the decision to not use the experimental data of ^{240}Pu as it was impossible to separate reasonably the fission fragments from the alpha pileup. In this section, we will discuss only the data related to ^{242}Pu isotope. We have used again, the spectrum of the spontaneous fission in order to check the stability of the detection efficiency of the photovoltaic cells during the measurements campaign. The discrepancy observed in Figure 4 between for example, the first and the second group points from the left, is explained by the change of both the MESYTEC linear amplifier and the shaping time. Indeed, changing the shaping time from 1µS to 0.25 µs permits a better separation between the events corresponding to alpha pileup of those corresponding to the fission fragments. However, we did not properly adjust the electronic threshold which is obviously too high, this is the reason why we obtain for the second group a low value for the measured efficiency. The third group is related to measurements with a detection threshold properly adjusted. Overall, the efficiency of the fission detector remains relatively stable at a value of 0.8, which is compatible with the efficiency calculated with the mass of the samples and the solid angle of the fission detector.

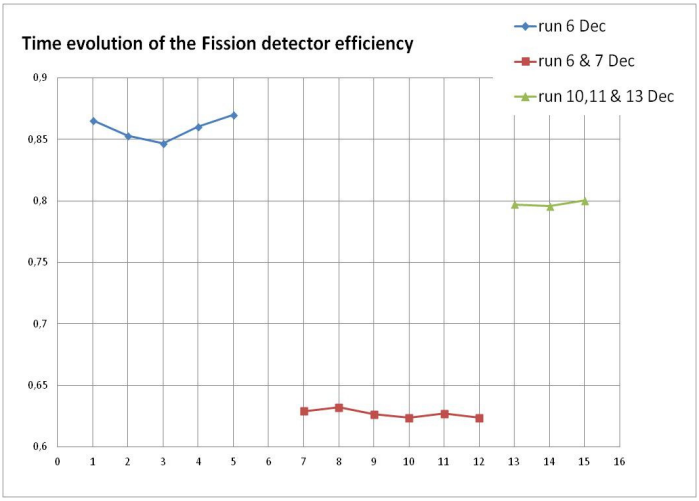

Figure 4. Time evolution of the fission detector efficiency for the ^{242}Pu isotope.

To determine properly the neutron flux impinging the PP film and then to infer the neutron flux at the ^{242}Pu target position, it is necessary to make two independent measurements of the scattered protons, in order to distinguish the protons emitted directly from the PP foil and those coming from side reactions of type (n, p) due to the materials surrounding the silicon detector. The subtraction requires a normalization factor which is provided by two independent neutron detectors monitoring

the neutron beam intensity. The figure 5 shows a comparison over the time of the ratio between the detected neutrons in the He_3 over those detected in the BF_3 detector. We expect, to have a small dependence with the neutron energy as the efficiencies of the two detectors could be different. However, the ratio should be constant at same neutron energy.

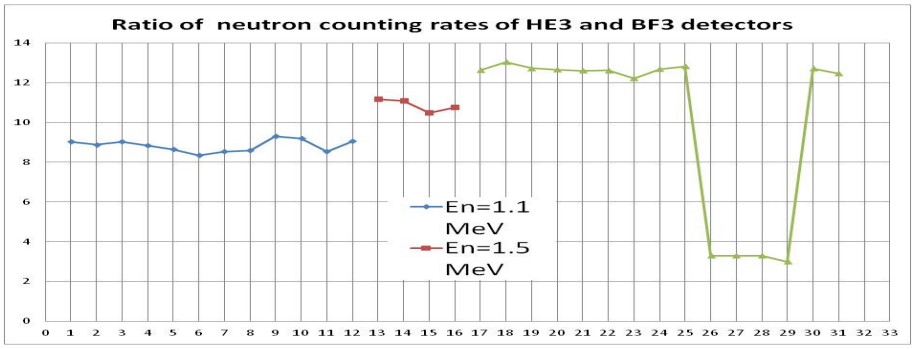

Figure 5 Dependence of He_3 and BF_3 neutron detector monitors with energy and beam intensity.

The observed variations in Figure 5 are outside statistical fluctuations. These variations are of the order of 5 - 10% at 1.1 MeV and up to 7% at 1.5 MeV. At 2 MeV, the fall of the counting rate observed for the He3 detector could be explained by an electronic malfunction of the SCALER module associated to this detector. In the following figures, 6a and 6b, we have plotted the ratio between the detected fission fragments which have been already corrected for the spontaneous fission (0.687 fission.s^{-1} or 0.798 fission.s^{-1} depending on the threshold adjustment) contribution and the number of neutrons detected by each neutron monitor.

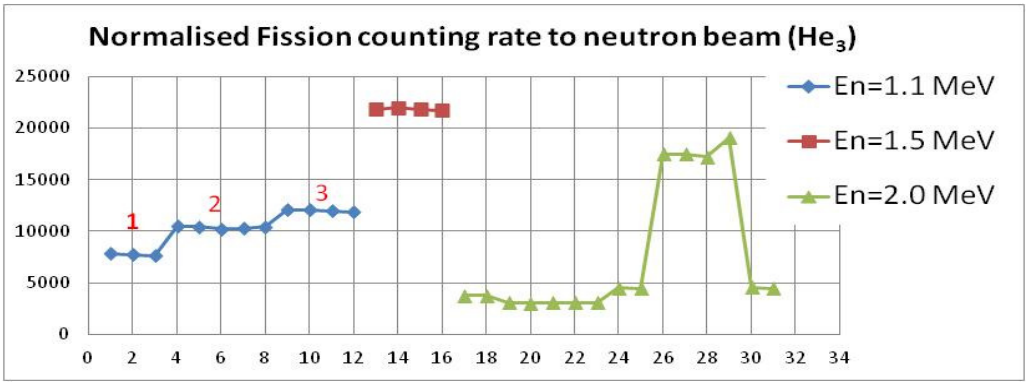

Figure 6a. Normalized fission events to the He_3 neutron detector

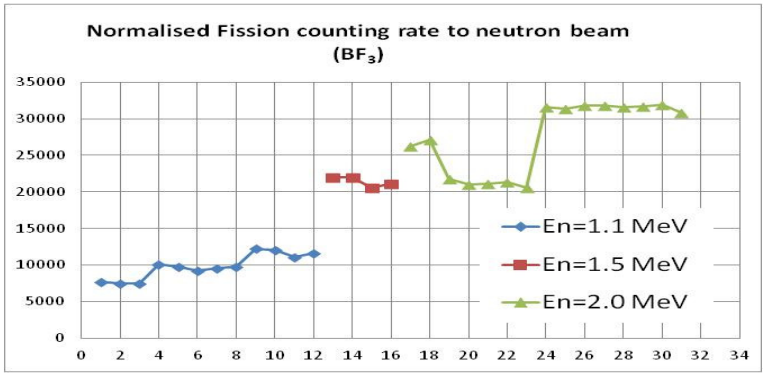

Figure 6b. Normalized fission events to the BF_3 neutron detector

At 1.1 MeV neutron energy, the figures 6a and 6b show three stages. The jump from step number 1 to the step number 2 is due to the electronic threshold which has been correctly adjusted after the step 1. The next jump could be explained by the modification of the cooling system which has been changed from water to air cooling. The MNCP simulations show that more neutrons are scattered with the water cooling system [35].

At 1.5 MeV, the normalization of the fission events to the He_3 neutron detector seems to be quite similar. Unfortunately, this is not the case when the same events are normalized to the BF_3 neutron detector. We didn't find any explanation to the observed discrepancy.

The situation is worst at 2 MeV where many unexplained variations appear between these fission events throughout the experiment. However, a relative stability is seen for the last measures normalized to the BF_3 neutron detector monitor.

The last concern of the present work is to examine the response of the silicon detector as a function of the energy of the incident neutrons. We performed the same work by checking the consistency of the recorded data for the detected protons spectra. We first verified the stability of the different measures of the recoil protons number detected at the same neutron energy. We have plotted in the Figure 7a and 7b, the counting rates observed with the silicon detector, normalized to the number of neutrons detected in both He_3 and BF_3 neutron monitors.

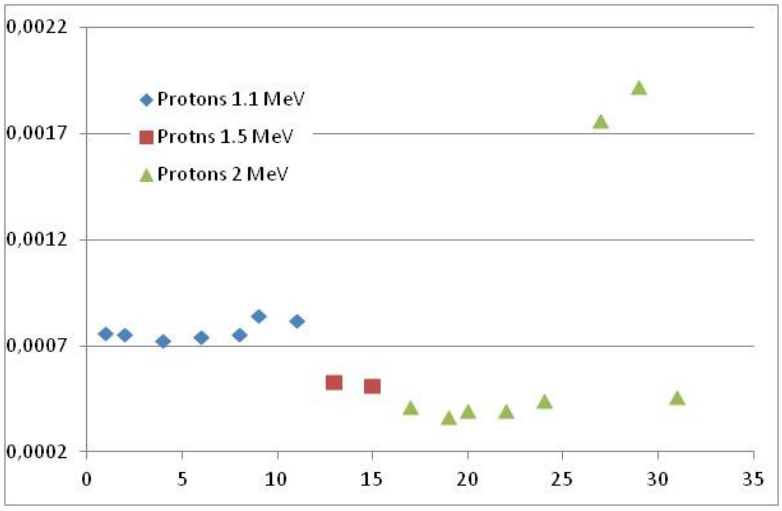

Figure 7a Normalized counting rate of the silicon detector to the He_3 neutron monitor.

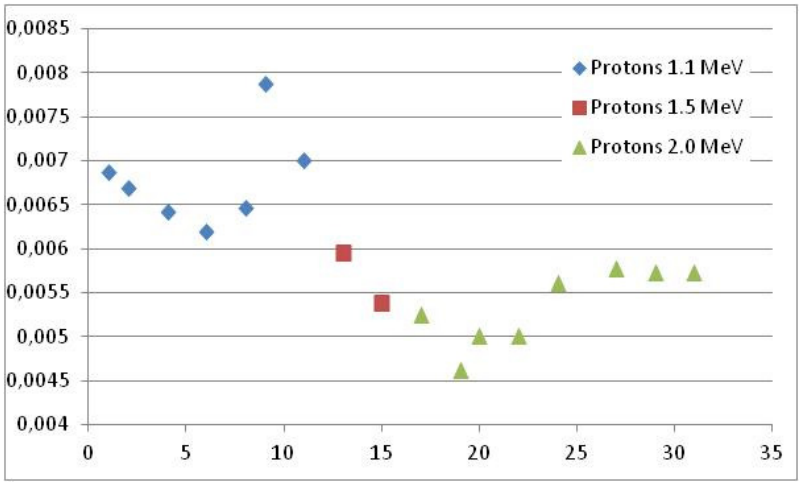

Figure 7b Normalized counting rate of the silicon detector to the BF_3 neutron monitor.

As for the fission events treatment, we observe also for 1.1 MeV neutron energy, many discrepancies which appear in the normalized counting rate with a maximum of 20-25%. These discrepancies remains unchanged either the data are normalized to the He_3 or to the BF_3 neutron detector. It may be noted that the last two measures at 1.1 MeV, correspond to the measurements made after changing the cooling system from water to air.

It is difficult to conclude on the stability of the measurements at 1.5 MeV, as we have only two measures. They present a discrepancy which is about 4%.

For the last series of measures at 2.0 MeV neutron energy, we observe important variations when the data are normalized to the He_3 neutron monitor. However, by normalizing the same data to the BF_3 neutron monitor, we can consider that the last three measures are stable in a limit of 0.2%. It seems therefore possible for these last three measures to determine the fission cross section for ^{242}Pu.

In the next figure 8, we have considered two measures: the recoil protons spectra related to the neutron energy of 2.0 MeV with and without the PP foil.

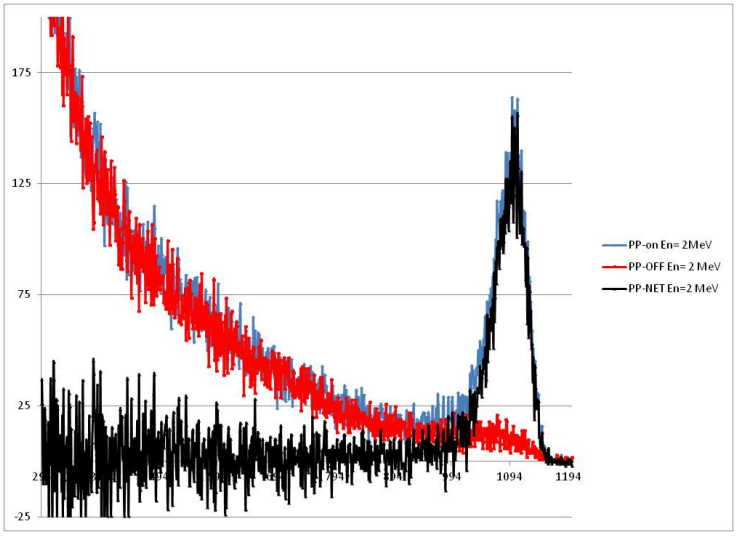

Figure 8 Recoil protons spectrum at an average energy of 2 MeV.

We have plotted the spectrum of the scattered protons from the PP foil (solid blue line) and superimposed the background spectrum generated by the (n,p) side reactions of the surrounding materials (solid red line). The resulting spectrum (solid black line), is obtained by subtracting the background events to the PP events, after a normalization of the two spectra by considering the number of neutrons detected in the BF_3 monitor for the two measures. The remaining protons in the spectrum are only those emitted from the polypropylene foil. The normalization factor seems to be correct, we observe a "normal" statistical fluctuations for the channels which are below the 2 MeV proton energy peak.

4.4 Conclusions

We have presented here the experiment aimed to measure for the first time, the fission cross section of ^{242}Pu in reference to the neutron-proton scattering cross section. The experimental data obtained for three neutron energies at 1.1, 1.5 and 2.0 MeV have been analysed in order to establish whether the neutron-induced fission cross section for ^{240}Pu and ^{242}Pu could be achieved. We have shown that

the solar cells used as a fission fragments detector, could resist against the damage caused by the alpha decay of the target with an upper limit of 0.2 MBq.

For the neutron flux measurement which is crucial for the reduction of the uncertainties on the measured cross sections, we have taken care to use two independent neutron detectors to monitor the neutron beam. Unfortunately, we had a malfunction of the SCALER electronic module, used to record the total neutron number for each measure. As a consequence, the determination of the neutron flux will be affected by a huge uncertainty, incompatible with the aimed goals. However, the count rates associated to the fission fragments and recoil protons when normalized to the BF_3 neutron monitor at 2 MeV neutron energy, will be considered for the last three measures as there variation is limited. It seems therefore possible for these last three measures to determine the fission cross section for ^{242}Pu.

The experience we have gained from this work will allow us to better prepare for the next experiment, which will aim to carry out these measures. In addition, we will pursue these measures by developing a proton recoil detector capable of detecting protons (neutrons) of 400 keV.

Aknowledgments

This work has been done with the financial support from the ANDES collaboration (contract FP7-249671) and ERINDA (contract FP7-269499) and CNRS programme PACE/GEDEPEON.

Bibliography

[1] G. Aliberti, G. Palmiotti, M. Salvatores, and C. G. Stenberg. Impact of nuclear data uncertainties on transmutation of actinides in accelerator-driven assemblies. *Nucl. Sci. Eng.*, 146:13, 2004.

[2] G. Aliberti, G. Palmiotti, M. Salvatores, T.K. Kim, T.A. Taiwo, M. Anitescu, I. Kodeli, E. Sartori, J.C. Bosq, and J. Tommasi. Nuclear data sensitivity, uncertainty and target accuracy assesment for future nuclear systems. *Ann. Nucl. Energy*, 33:700, 2006.

[3] Nuria Garcia-Herranz, Oscar Cabellos, Javier Sanz, Jesus Juan, and Jim C. Kuijper. Propagation of statistical and nuclear data uncertainties in monte carlo burn-up calculations. *Ann. Nucl. Energy*, 35:714, 2008.

[4] M. Salvatores, coordinator. Uncertainty and target accuracy assessment for innovative systems using recent covariance evaluations. Organisation for Economic Co-operation and Development, Nuclear Energy Agency, International Evaluation Co-operation, Volume-26, NEA/WPEC-26, ISBN 978-92-64-99053-1, 2008.

[5] N. Garcia-Herranz, O. Cabellos, F. Alvarez-Velarde, J. Sanz, E.M. Gonzalez-Romero, and J. Juan. Nuclear data requirements for the ads conceptual design efit: Uncertainty and sensitivity study. *Ann. Nucl. Energy*, 37:1570, 2010.

[6] Working Party on International Evaluation Co-operation. The High Priority Request List for nuclear data (HPRL). NEA Nuclear Science Commitee, www.nea.fr/dbdata/hprl/, 2010.

[7] A.J.M. Plompen. Minor actinides, major challenges, the needs for and benefits of international collaboration. *Nucl. Data Sheets*, 115:to be published, 2013.

[8] M. Salvatores. *Uncertainty and Target Accuracy Assessment for Innovative Systems Using Recent Covariance Data Evaluations (NEA/WPEC-26)*. Nuclear Energy Agency (OECD), 2008.

[9] G. Sibbens, A. Moens, R. Eykens, D. Vanleeuw, F. Kehoe, H. Kühn, R. Wynants, J. Heyse, A. Plompen, R. Jakopiĉ, S. Richter, and Y. Aregbe. Preparation of ^{240}pu and ^{242}pu targets to improve cross section measurements for advanced reactors and fuel cycles. *J. Rad. Nucl. Chem.*, 297:DOI 10.1007/s10967–013–2669–6, 2013.

[10] P. Salvador-Castiñeira, T. Bryś, R. Eykens, F.-J. Hambsch, A. Moens, S. Oberstedt, C. Pretel, G. Sibbens, D. Vanleeuw, and M. Vidali. *accepted in Phys. Rev. C*, 2013.

[11] C. Budtz-Jørgensen and H.-H. Knitter. *Nucl. Sci. Eng.*, 86:10–21, 1984.

[12] Glenn F. Knoll. *Radiation Detection and Measurement*. John Wiley and Sons, Inc., New York, USA, third edition edition, 2000.

[13] J. F. Ziegler, J.P. Biersack, and M.D. Ziegler. SRIM The stopping and range of ions in matter. www.srim.org, SRIM Co., Chester, MD 21619, USA, ISBN 0-9654207-1-X, 2008.

[14] http://geant4.web.cern.ch/geant4/.

[15] K.-H. Schmidt and B. Jurado. Gef-code version 2012/2.7. http://www.cenbg.in2p3.fr/-GEF-/.

[16] N.E. Holden and D.C. Hoffman. *Pure Appl. Chem*, 72:1525–1562, 2000.

[17] M. B. Chadwick et al. ENDF/B-VII.1 Nuclear data for science and technology: Cross sections, covariances, fission product yields and decay data. *Nucl. Data Sheets*, 112:2887, 2011.

[18] C Paradela, L Tassan-Got, L Audouin, B Berthier, I Duran, L Ferrant, S Isaev, C Le Naour, C Stephan, D Tarrío, et al. Neutron-induced fission cross section of^{234} u and^{237} np measured at the cern neutron time-of-flight (n_tof) facility. *Physical Review C*, 82(3):034601, 2010.

[19] RJ Jiacoletti, WK Brown, and HG Olson. Fission cross sections of ^{237}np from 20 ev to 7 mev determined from a nuclear-explosive experiment. Technical report, Los Alamos Scientific Lab., N. Mex., 1972.

[20] U. Abbondanno et al. Tech. Rep. CERN-SL-2002-053 ECT, CERN, Geneva, 2002.

[21] C. Guerrero et al. *Eur. Phys. J. A*, 49:1, 2013.

[22] E. Berthoumieux. cds.cern.ch/record/1514680?ln=en.

[23] G. Sibbens, A. Moens, R. Eykens, D. Vanleeuw, F. Kehoe, H. Kühn, R. Wynants, J. Heyse, A. Plompen, R. Jakopic, S. Richter, and Y. Aregbe. Preparation of ^{240}Pu and ^{242}Pu targets to improve cross-section measurements for advanced reactors and fuel cycles. *J. Radioanal. Nucl. Chem., doi: 10.1007/s10967-013-2668-7*, 2013.

[24] Y. Giomataris et al. *Nucl. Instrum. Meth. A*, 376:29, 1996.

[25] N. Colonna et al. A software compensation technique for fission measurements at spallation neutron sources. Under preparation.

[26] A. Ferrari et al. Tech. Rep. CERN 2005-10, INFN/TC_05/11, SLAC-R-773, 2005.

[27] G. Battistoni et al. *AIP Conf. Proc.*, 896:31, 2007.

[28] E. Gonzalez-Romero (ed.) Report of the Numerical results from the Evaluation of the nuclear data sensitivities, Priority list and table of required accuracies for nuclear data, Deliverable D5.11 from IP-EUROTRANS.

[29] J.C Hopkins and G. Breit *Nucl. Data Tables*, A9:137, 1971.

[30] A.B. Laptev Proc. 4th Int. Conf. on Fission and Prop. of Neut. Rich nuclei, Sanibel Island, Florida, November 2007 (World Scientific, Singapore 2008)

[31] F. Tovesson *et al. Phys. Rev. C* 79:014613, 2009.

[32] G. Siegert *Nucl. Instr. and Meth.*, 164:437, 1979.

[33] G. Kessedjian *et al. Phys. Rev. C* 85:044613, 2012.

[34] C. Grosjean Ph.D thesis, Université de Bordeaux, 2005.

[35] Private communication.

European Commission
EUR 26200 EN – Joint Research Centre – Institute for Reference Materials and Measurements

Title: Fission cross section measurements for ^{240}Pu, ^{242}Pu – Deliverable 1.5 of the ANDES project

Author(s): P. Salvador-Castiñeira, A. Tsinganis, M. Aiche, S. Andriamonje, G. Belier, E. Berthoumieux, G. Boutoux, T. Brys, M. Calviani, S. Czajkowski, N. Colonna, Q. Ducasse, R. Eykens, C. Guerrero, F. Gunsing, F.-J. Hambsch, B. Jurado, G. Kessedjian, C. Massimi, L. Mathieu, J. Mattaranz, A. Moens, S. Oberstedt, A.J.M. Plompen, C. Pretel, G. Sibbens, J. Taieb, D. Vanleeuw, M. Vidali, V. Vlachoudis, R. Vlastou, the n_TOF Collaboration

Luxembourg: Publications Office of the European Union

2013 – 36 pp. – 21.0 x 29.7 cm

EUR – Scientific and Technical Research series – ISSN 1831-9424 (online)

ISBN 978-92-79-33002-5 (pdf)

doi: 10.2787/81004 (pdf)

Abstract

This report comprises the deliverable 1.5 of the ANDES project (EURATOM contract FP7-249671) of Task 1.3 “High accuracy measurements for fission” of Work Package 1 entitled "Measurements for advanced reactor systems". This deliverable provides evidence of a successful completion of the objectives of Task 1.3.

LA-NA-26200-EN-N

As the Commission's in-house science service, the Joint Research Centre's mission is to provide EU policies with independent, evidence-based scientific and technical support throughout the whole policy cycle.

Working in close cooperation with policy Directorates-General, the JRC addresses key societal challenges while stimulating innovation through developing new standards, methods and tools, and sharing and transferring its know-how to the Member States and international community.

Key policy areas include: environment and climate change; energy and transport; agriculture and food security; health and consumer protection; information society and digital agenda; safety and security including nuclear; all supported through a cross-cutting and multi-disciplinary approach.

Publications Office

ISBN 978-92-79-33002-5